Probing the Abundance Ratios of Comets using Fabry-Pérot Observations

J. P. Morgenthaler, W. Harris, F. Scherb, F. L. Roesler, N. E. Doane, (University of Wisconsin), R. J. Oliversen (GSFC), M. R. Combi (U. Mich.), M. L. Marconi (FPRI), W. H. Smyth (AER)

Outline

- Introduction: what are comets and why do we care
- Scheme for deriving abundance ratios from wide-field observations of comets
- Progress
  - Measure and model $\mathrm{H_2O}$ daughters OH 3080 Å, $\mathrm{H}\alpha$, [O I] 6300 Å
    - standard OH photodissociation rates are likely wrong
    - see puzzling tailward asymmetry
  - Measure CO photodissociation product [C I] 9850 Å
    - [C I] 9850 Å is likely not just a photodissociation product, at least in Hale-Bopp
- To do

Where do comets come from?

- The primordial solar nebula
- Nebular collapse, planetary formation
- Dynamical things happen, planet orbits change, etc.
- Leftover planetesimals
  - Rocky asteroids (2–3.5 AU)
  - Icy Kuiper belt objects (50–500 AU)
  - Oort cloud objects (500–50,000 AU)
    - dynamically ejected by planets
    - primordial
    - interstellar
- Dynamical evolution
- Apparition

What does a comet look like?

Based on what we see coming off of comets, they are:

- Mostly water
- 5–15% CO
- $\lesssim 5\%\ \mathrm{CO_2}$
- $\lesssim 1\%$ Other molecules, including organics
- $\sim 10\%$ "dust"
  - may or may not be similar to interstellar dust
  - (as if interstellar dust has any typical form)
- More-or-less homogeneous
  - comet fragments look like comets
- **Dirty snowballs**

What happens to comets when they get close to the sun?

- H_2O, CO, other volatiles sublime
  - Form coma
    - more-or-less spherical distribution of gas
    - density ranges from near atmospheric to interplanetary
    - like a planetary atmosphere without gravity
  - Ion tail
    - solar radiation and charge exchange with solar wind ions ionizes some coma gas
    - ions accelerated by solar wind
    - acceleration moderated by collisions with neutrals
- Dust is liberated
- Comet nucleus often splits
  - Is there a continuous size distribution from dust grain through comet fragment?
- Comets evolve over many perihelion passages

Fig. 1.— Comet Hale-Bopp image courtesy of H. Mikuz & B. Kambic (http://www.amtsgym-sdbg.dk/as).

Why study comets?

- Choose your favorite topic:
  - Observational challenge: it moves
  - Present day solar system dynamics
  - Coma physics
    - atmospheric physics
    - atomic and molecular physics
  - Surface physics
    - nucleus
    - dust
- Cometary composition can help answer questions about:
  - Solar nebula
  - Planetary formation
  - Dynamical history

How should we study comets

- In all wavebands
  - Radio through X-ray
  - Molecular rotation/vibration to charge exchange reactions with solar wind ions
- At many resolutions
  - Continuum solar radiation scattered from dust
  - Abundance studies
  - Line profiles for dynamics
- Polarization
- At many angular scales
  - Nucleus structure (< 20 km)
  - 0.5 AU diameter $\mathrm{Ly}\alpha$ coma

The UW/GSFC Hale-Bopp observing campaign

- Large campaign, PI Frank Scherb (Scherb *et al.* 1997; Morgenthaler *et al.* 2002)
- IR, optical, UV
- Sub arcsec using Mt. Wilson AO to 1° using WHAM and Burrell Schmidt
- UV imaging spectropolarimetry with WISP sounding rocket
- HPOL 3200 Å-10,500 Å
- Resolving powers ($\lambda/\Delta\lambda$) from broad-band filters to 60,000
- **Wide-field high resolving power using Fabry-Pérot spectrometers**

Scheme for deriving abundance ratios from wide-field observations of comets

- Material outgasses from comet forming the coma
- Coma interacts with sunlight, dissociating and/or fluorescing
- Count all the photons produced in a few key lines
- Understand how photons relate to parent population
- Understand how outgassing rates relate to intrinsic abundance ratios
- Derive abundance ratios
- **Need sensitive wide field high resolution spectrometry and imaging**

Water and carbon monoxide

- Comets are mostly water, 5–15% CO and $\lesssim 5\%\ \mathrm{CO_2}$
- UV sunlight photodissociates water into H, OH, H_2, O (Table 1)
- Lines studied in this work: $\mathrm{H}\alpha$, OH 3080Å, [O I] 6300 Å, [C I] 9850 Å
- $\mathrm{H}\alpha$, OH 3080Åexcited by solar UV light (fluorescence)
- [O I], [C I] are not fluorescent: photodissociation products or collisionally excited

Table 1. Photodissociation Branching Ratios

Reaction	BRn	Quiet Sun	Active Sun	Ref.[a]
$\mathrm{H_2O} + h\nu \rightarrow \mathrm{H_2} + \mathrm{O}(^1D)$	BR1	0.050	0.067	H
$\mathrm{H_2O} + h\nu \rightarrow \mathrm{H} + \mathrm{OH}$	BR2	0.855	0.801	H
$\mathrm{OH} + h\nu \rightarrow \mathrm{H} + \mathrm{O}(^1D)$	BR3	0.094	$\cdots$	M
$\mathrm{OH} + h\nu \rightarrow \mathrm{H} + \mathrm{O}(^1D)$	BR3$'$	0.357	$\cdots$	M
$\mathrm{OH} + h\nu \rightarrow \mathrm{H} + \mathrm{O}(^3P)$	BR4	0.662	0.513	V
$\mathrm{OH} + h\nu \rightarrow \mathrm{H} + \mathrm{O}(^3P)$	BR4$'$	0.472	$\cdots$	M
$\mathrm{CO}(X^1\Sigma^+) + h\nu \rightarrow \mathrm{C}(^1D) + \mathrm{O}(^1D)$	BR5	0.046	0.042	H
$\mathrm{CO}(X^1\Sigma^+) + h\nu \rightarrow \mathrm{C}(^1D) + \mathrm{O}(^1D)$	BR5$'$	0.123	0.123	T
$\mathrm{CO_2} + h\nu \rightarrow \mathrm{CO}(X^1\Sigma^+) + \mathrm{O}(^1D)$ ..	BR6	0.457	0.391	H

[a]H, Huebner *et al.* (1992); V, van Dishoeck & Dalgarno (1984); M Morgenthaler *et al.* (2001); T Tozzi, Feldman, & Festou (1998). The van Dishoeck & Dalgarno OH cross sections have been calculated for a heliocentric velocity of -14 $\mathrm{km\ s^{-1}}$, appropriate for 1997 early March.

Wide field Fabry-Pérot (FP) observations

- Telescopes
  - WHAM (fig. 2)
  - McMath-Pierce Solar telescope on Kitt Peak, Arizona (figs. 3–4)
- Instruments
  - WHAM: 150 mm dual etalon Fabry-Pérot spectrometer, FOV=60′ operated in spectral and imaging modes
  - McMath-Pierce: 50 mm dual etalon Fabry-Pérot spectrometer, FOV=4′.1 operated in spectral mode
  - FP (ring) images recorded onto CCDs

Fig. 2.— The Wisconsin Hα Mapper (WHAM) at Kitt Peak National Observatory (http://www.astro.wisc.edu/wham).

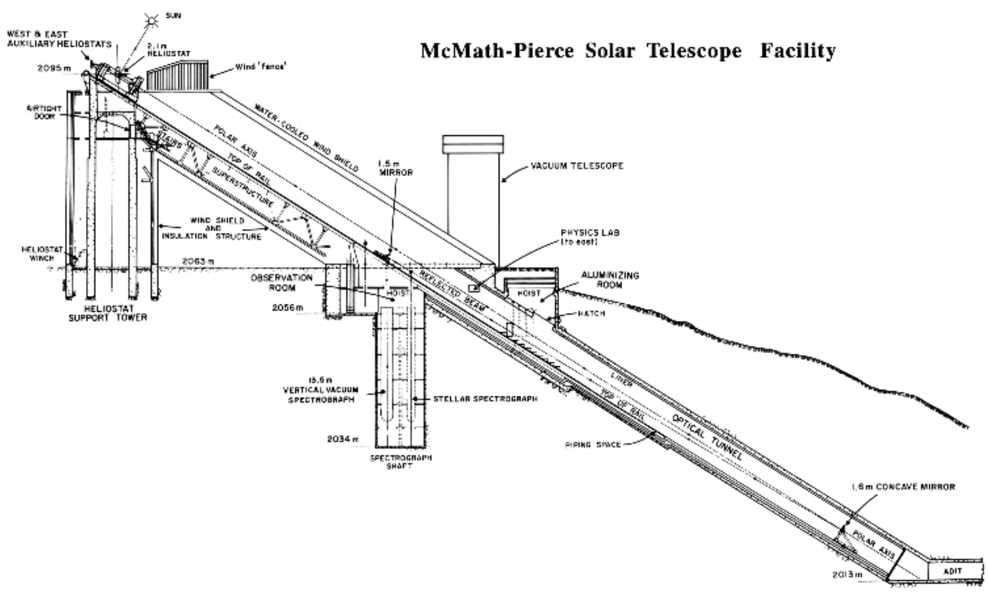

Fig. 3.— McMath-Pierce Solar telescope. Figures courtesy of NOAO/ AURA/NSF.

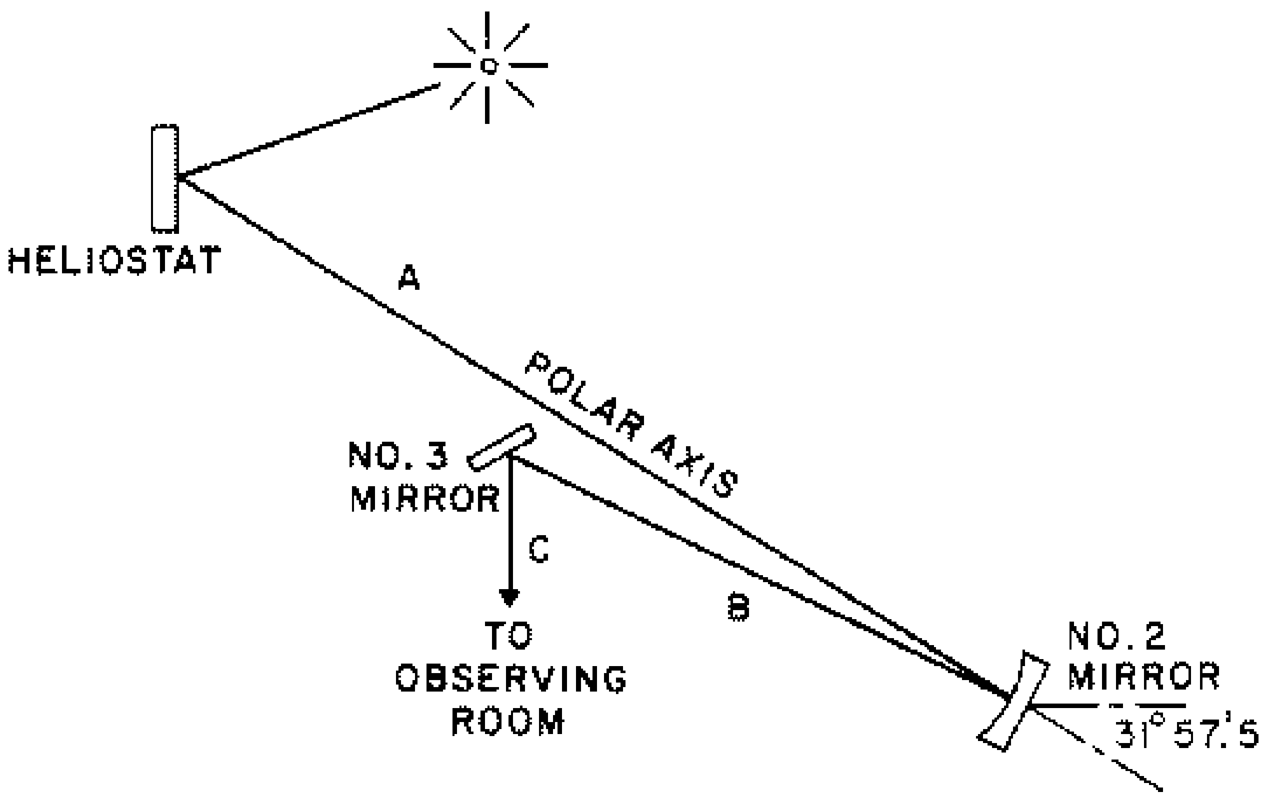

Fig. 4.— McMath-Pierce Solar telescope light path. Figure courtesy of NOAO/AURA/NSF.

Fabry-Pérot review (Roesler 1974)

- One etalon = two parallel, reflective plates of glass
- Spacing between plates = D, wavelength of light λ determine angle of transmission, θ for order m:

$$\cos(\theta) = \frac{m\lambda}{2D} \tag{1}$$

- Ideal transmission given by Airy function
- Spacing between plates can be varied by changing the pressure of a high index of refraction gas (SF_6)
- Multiple etalons used to increase resolving power
- Much larger input solid angle than diffractive spectrographs at the same resolving power
- Large apertures (2-6 inches) mean phenomenal sensitivity
- Ideal for faint diffuse sources like cometary comae

OH 3080 Å observations

- Narrow-band large-aperture (1°) OH 3080 Å filter images taken with Burrell Schmidt telescope on Kitt Peak
- Tracked OH emission to cometocentric distances of 1×10^6 km
- Aperture summation photometry and OH fluorescent efficiency (g factor) gives coma model independent OH production rate, Q(OH)
- Data not consistent with single velocity spherical outflow (Haser 1957) models–implies accelerating flow (Harris *et al.* 2002)

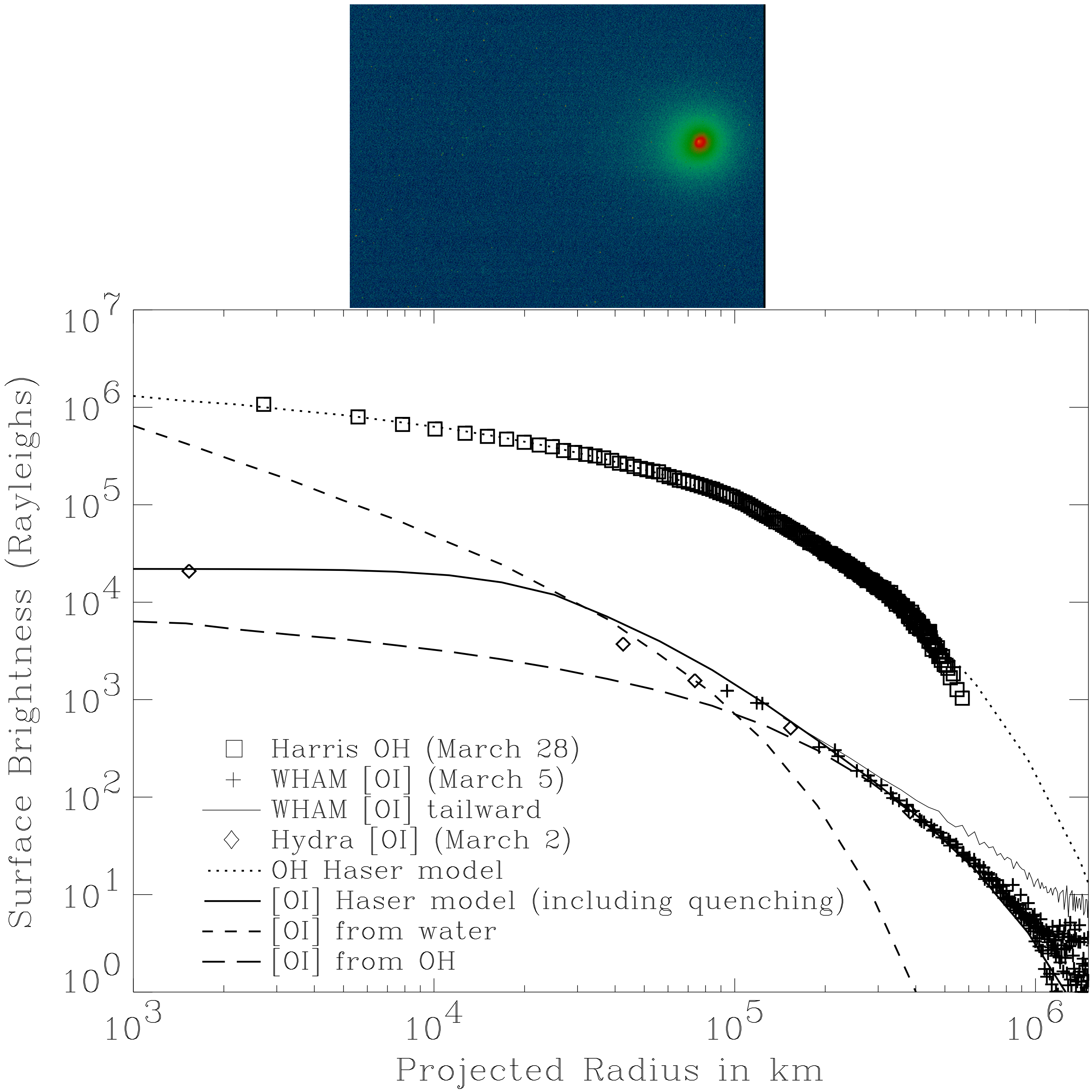

Fig. 5.— The OH 3080 Å emission image was recorded at the Kitt Peak Burrell Schmidt telescope UT 1997 April 8 and used to make the average OH radial profile shown as the top set of data points on the graph.

FP spectra of Hale-Bopp in [O1] 6300 Å

- 1° FOV covers entire [O I] coma
- Aperture summation gives total $\mathrm{O}(^1D)$ production rate

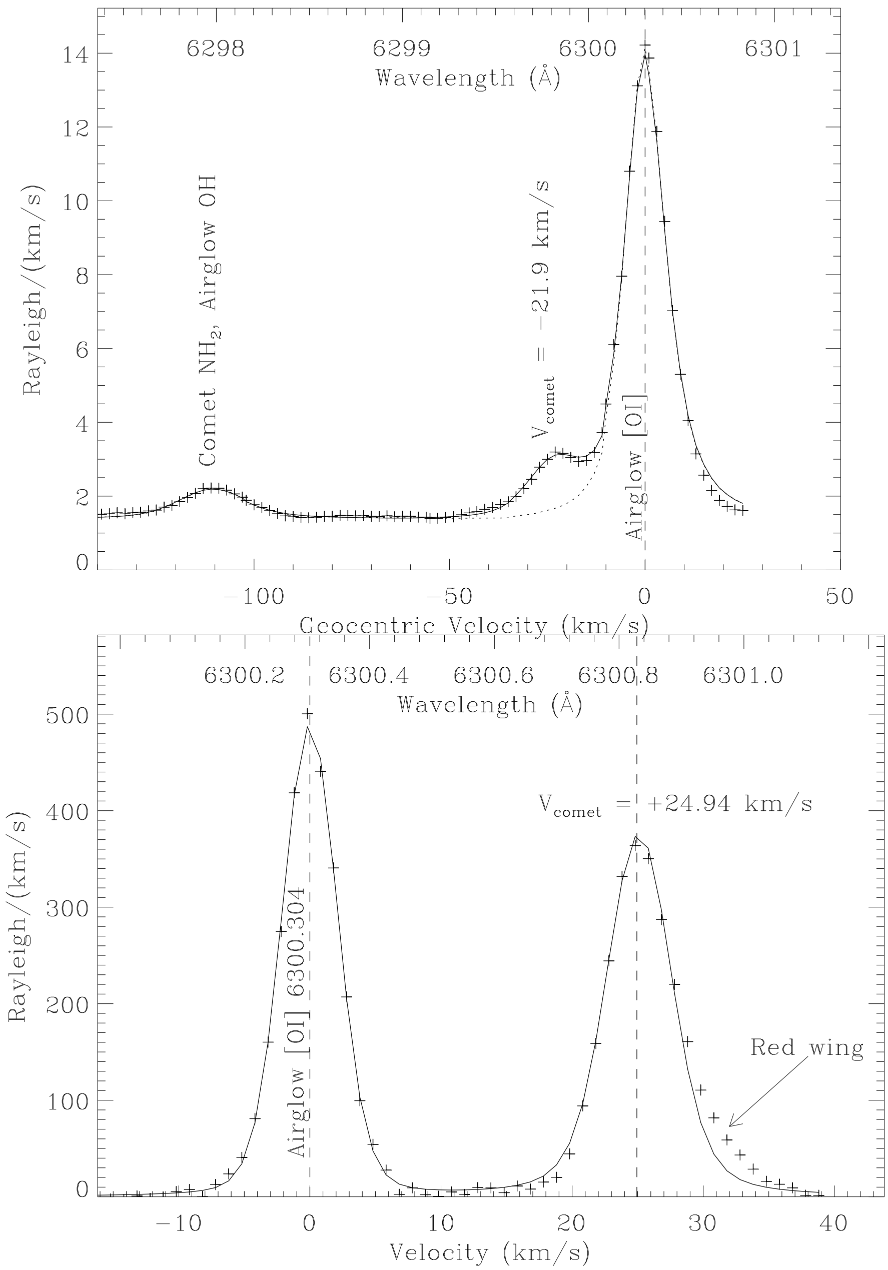

Fig. 6.— FP spectra of comet Hale-Bopp. WHAM 1997 March 5 (left) and 50 mm FP 1997 April 14 (right).

[O1] 6300 Å Spatial Information

- WHAM images, WIYN Hydra and Densepak spectra
- Shows unexpected asymmetry (see below)
- Radial profiles of [O I] distribution indicates OH branching ratio more likely cause of large [O I] production than H_2O branching ratio

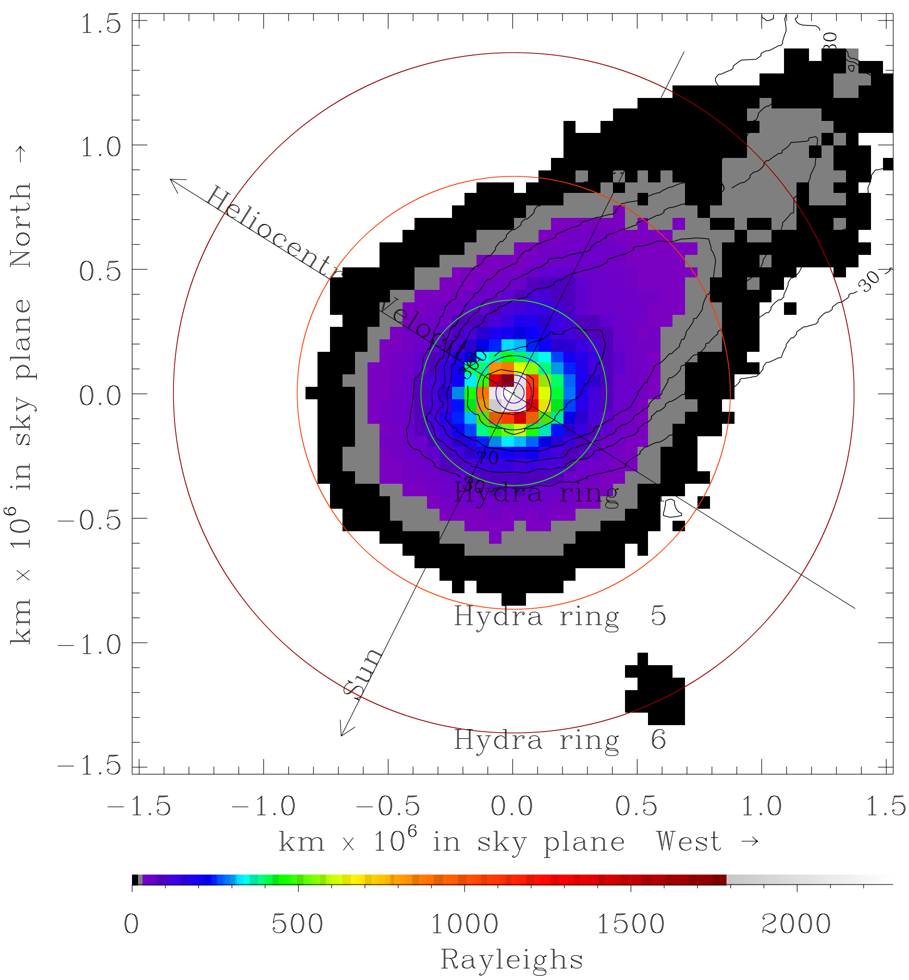

Fig. 7.— Hale-Bopp 1997 March 5 image with [O I] emission shown in gray scale, dust in contours, and circles showing positions of the Hydra annuli. The asymmetry accounts for ∼13% of the [O I] emission.

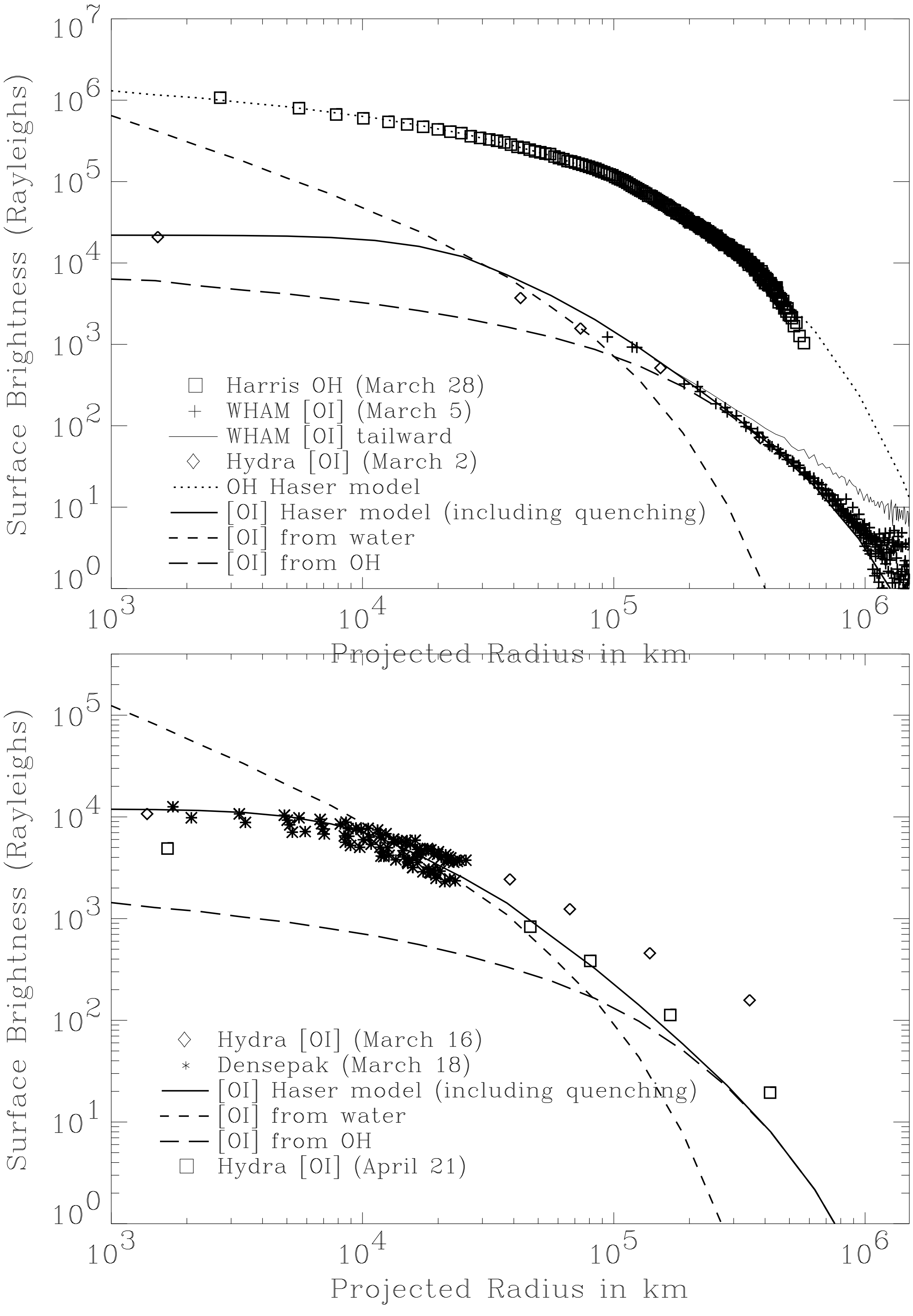

Fig. 8.— [O I] 6300 Å radial profiles from WHAM and WIYN MOS data plotted with OH radial profile (top).

Water production rate history

- OH 3080 Å (Harris *et al.* 2002), OH radio (e.g. Colom *et al.* 1999), Lyα (Combi *et al.* 2000), H_2O IR (Dello Russo *et al.* 2000) [O I] 6300 Å used to derive Q(H_2O)
- Problem [O I] measurements give Q(H_2O) rates that are high by a factor of 3–4 (fig. 9)
- Likely solution to the problem: standard theoretical OH cross section at Lyα (van Dishoeck & Dalgarno 1984) probably too small
- Nee & Lee (1984) measured cross section at Lyα fixes the problem
- Problem with this solution: Nee & Lee cross section too high everywhere else

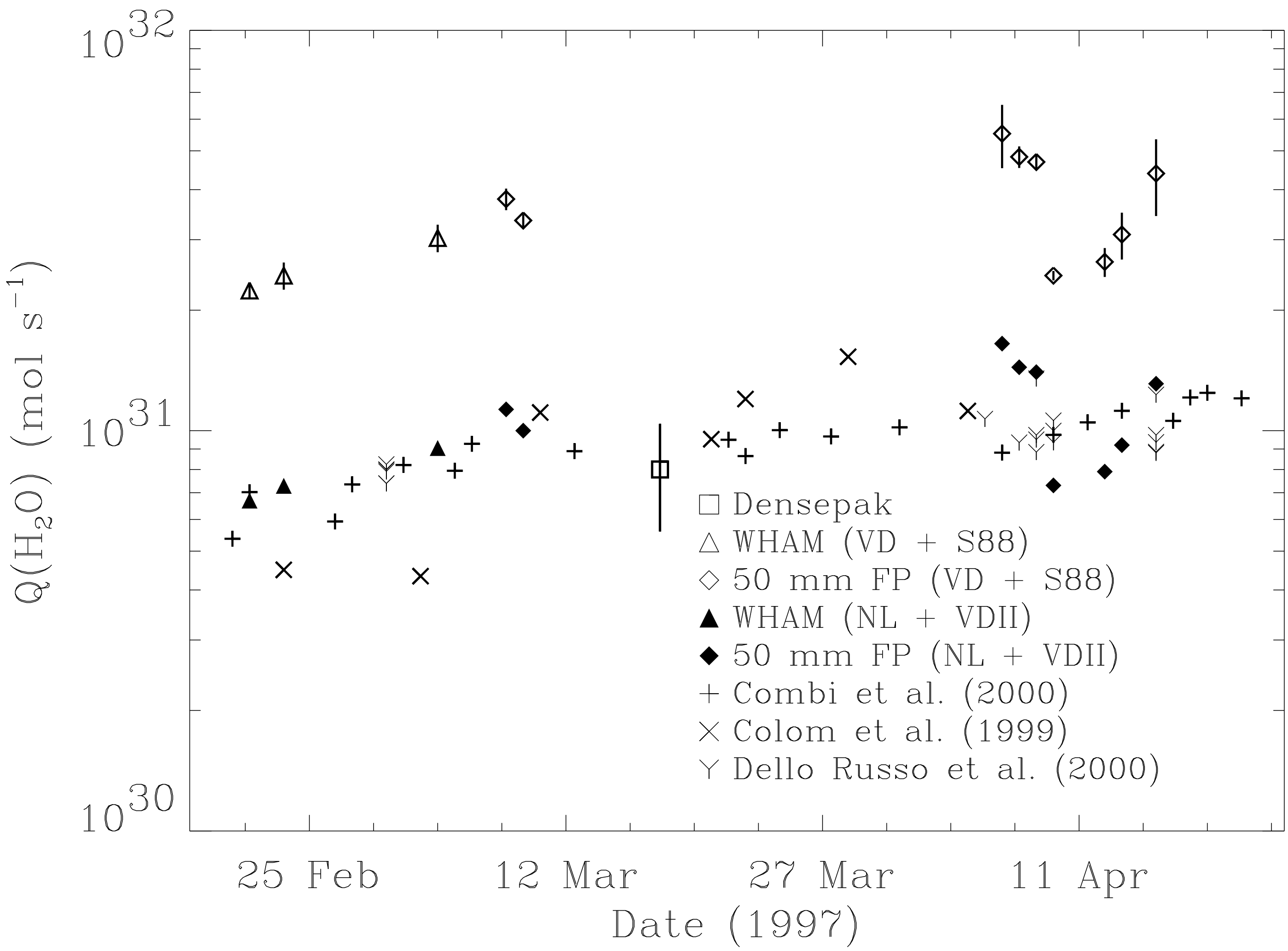

Fig. 9.— Q(H_2O) values from various works. Open symbols denote production rates derived with the standard OH $\rightarrow$ $O(^1D)$ branching ratio. Filled symbols are the same but with the branching ratio from Morgenthaler *et al.* (2001).

Tailward Asymmetry seen in OH and [O1] 6300 Å

- Between ion and dust tails
- Possibly neutrals accelerated by ions (Harris *et al.* 2002)
- Some tailward [O I] might be caused by collisional excitation (analysis not complete)
- OH probably not caused by an extra source

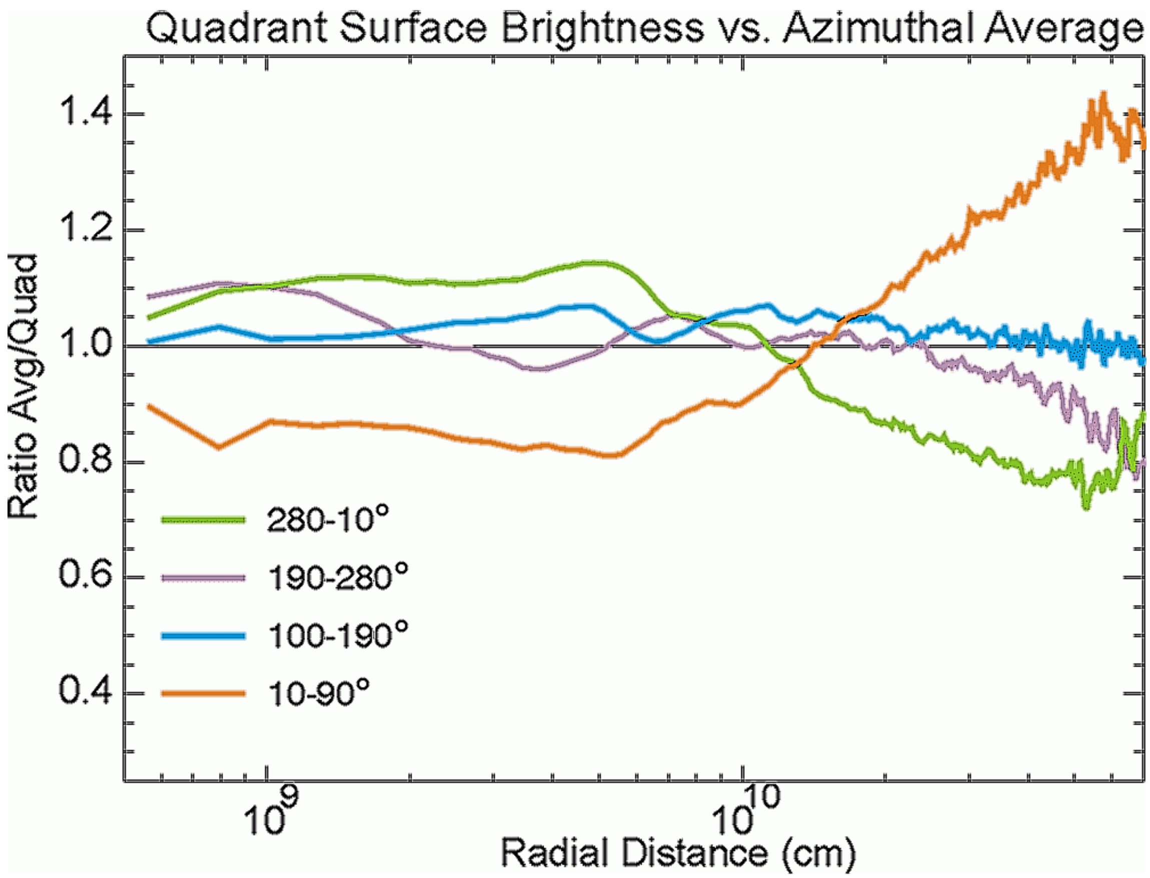

Fig. 10.— Quadrant-by-quadrant variation of the OH radial profile from its azimuthally averaged value, where the tailward quadrant is 10–100° (Harris *et al.* 2002).

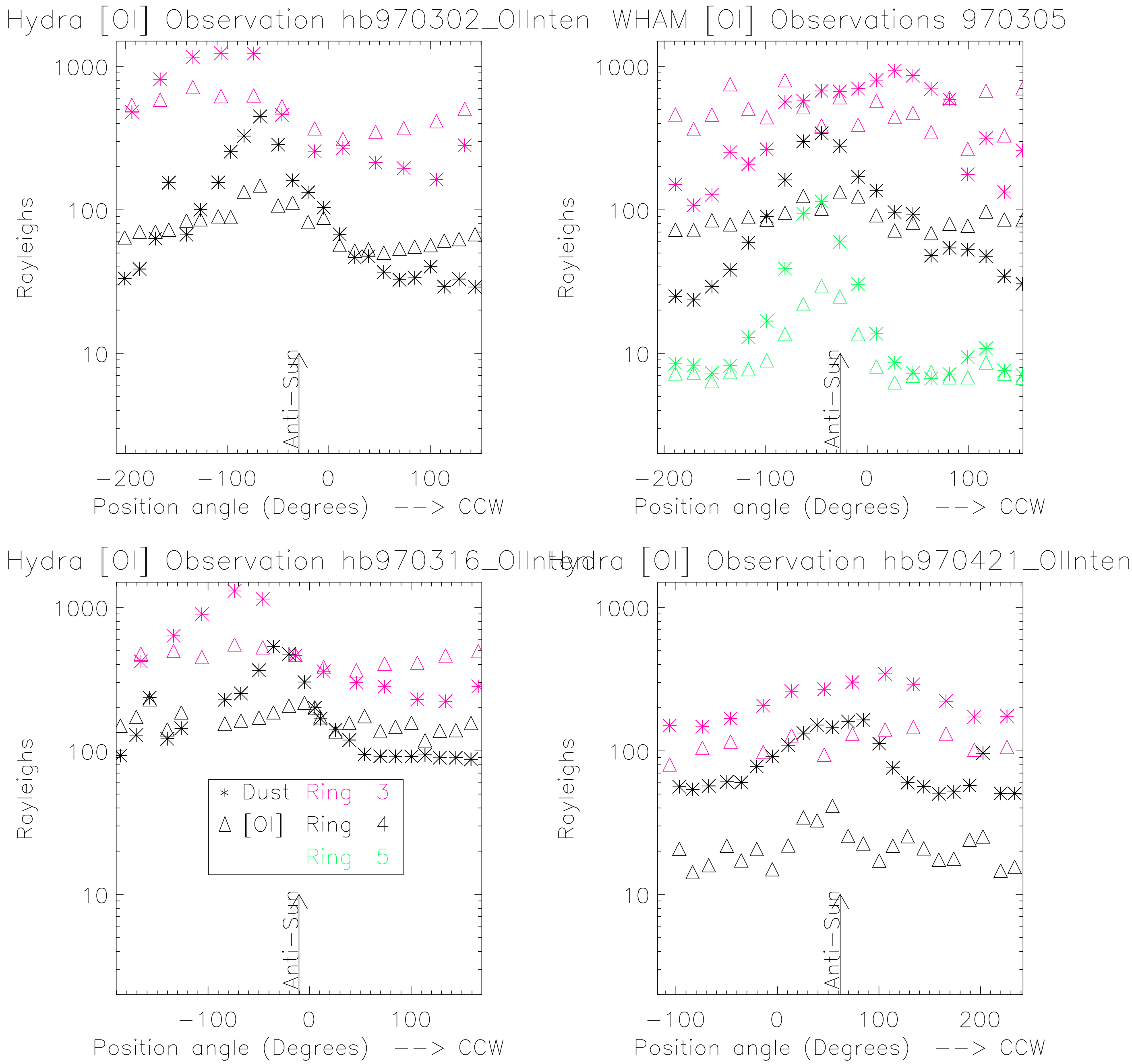

Fig. 11.— Comparison of WHAM and Hydra [O I] data. The black triangles show the azimuthal distribution of the [O I] surface brightness at a radius of 6 arcminutes (∼360,000 km) is peaked between the dust tail and the ion tail.

Hα observations

- High resolving power 50mm FP at the McMath-Pierce solar telescope
- $4'.1$ FOV centered $\sim 5'$ sunward of nucleus to avoid H_2O^+ line
- Currently completing reduction
- Preliminary results: line widths narrower than comet Halley implies faster collisional thermalization of fast H atoms (dissociation products) in Hale-Bopp's dense coma
- Monte Carlo model of coma that includes opacity effects for solar Lyα needed to properly interpret line profiles

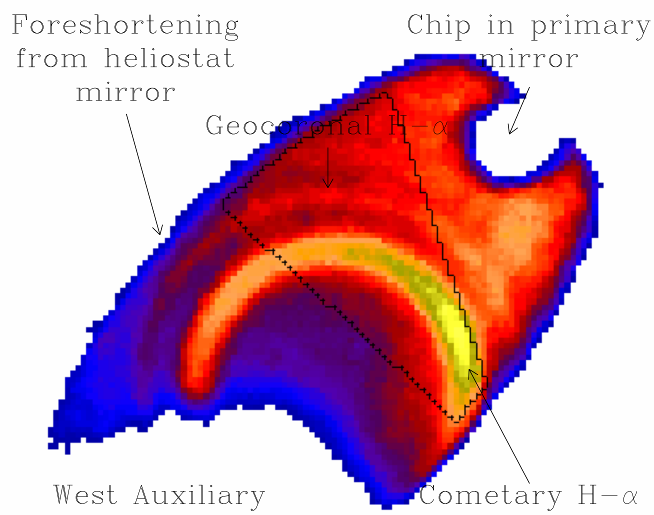

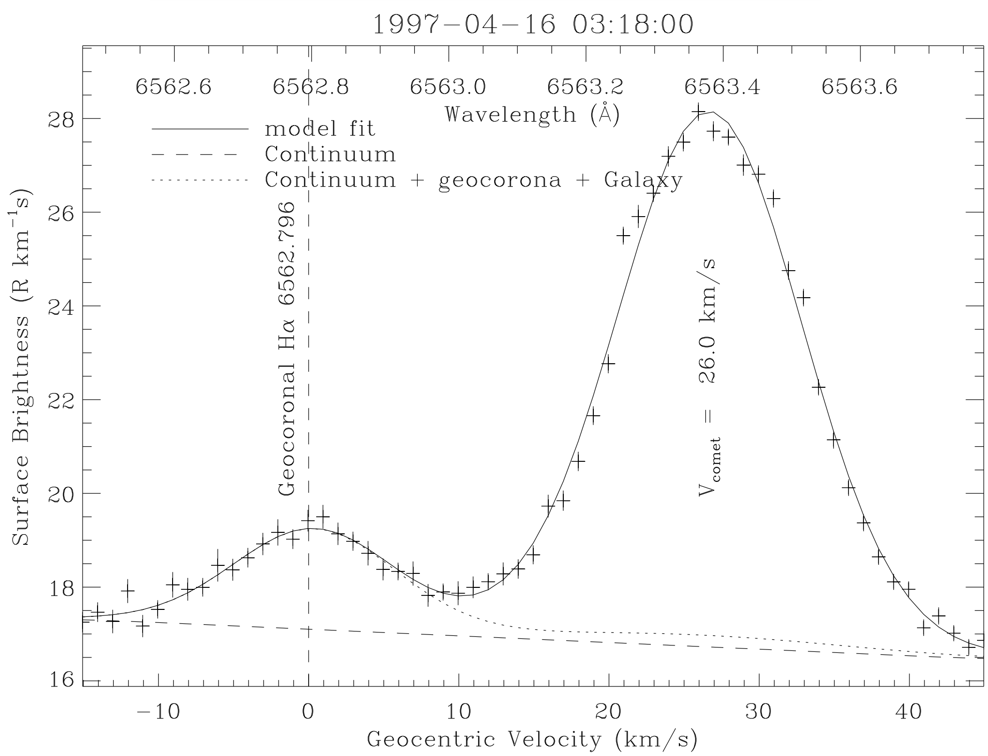

Fig. 12.— Fabry-Pérot (FP) ring image and spectrum of Hale-Bopp in Hα recorded UT 1997 April 16 03:18. The outline shows the section of the image used to make the spectrum. The spectrum is fit with two variable Gaussians, a sloping continuum and two fixed Gaussians for the Galaxy.

[C1] 9850 Å observations

- 50mm FP at the McMath-Pierce solar telescope
- Crude mapping shows radial distribution not consistent with photodissociation source
- Need collisional excitation calculations to fully interpret

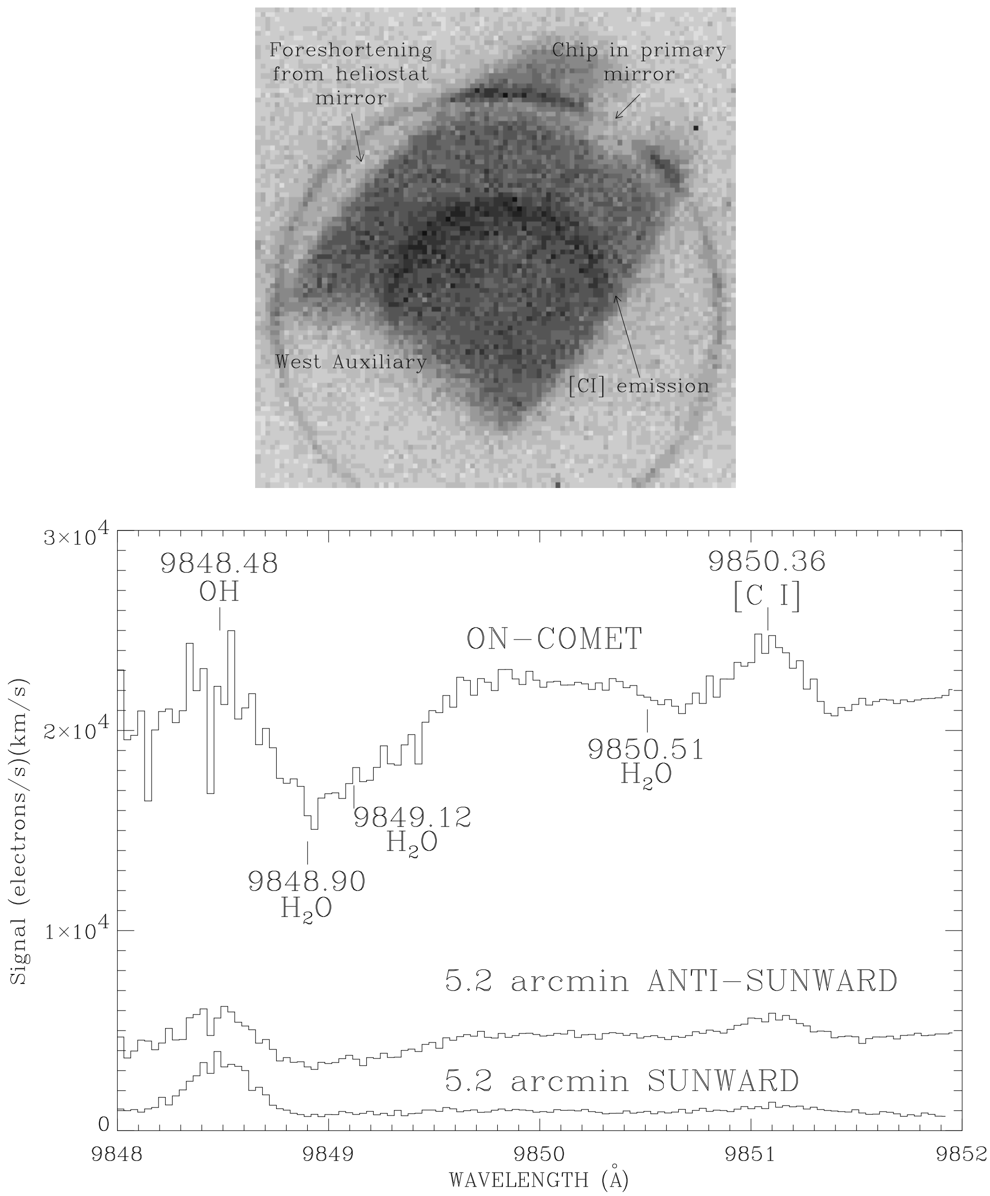

Fig. 13.— Example [C I] 9850 Å Fabry-Pérot ring image (top) showing the [C I] emission line. The ring that extends beyond the mirror image is terrestrial OH 9848.48 Å reflecting off the heliostat superstructure.

To Do

- Produce global coma models incorporating all known coma physics
  - currently modeling is done piece-meal: a hydro code here, a Monte-Carlo code there, etc.
- Use data to constrain models, finding which atomic and molecular constants need more lab study
- Only model free parameters should be outgassing rates of major species
- Figure out relation between intrinsic composition and outgassing rates
- Derive intrinsic abundances
- Repeat for all observable comets over as many perihelion passages as possible
- Use abundance data to reconstruct evolution of solar nebula

REFERENCES

Colom, P., Gérard, E., Crovisier, J., & Bockelée-Morvan, D. 1999, Earth, Moon, Planets, 78, 37

Combi, M. R., Reinard, A. A., Bertaux, J., Quemerais, E., & Mäkinen, T. 2000, Icarus, 144, 191

Dello Russo, N., Di Santi, M. J., Magee-Sauer, K., Novak, R., & Rettig, T. W. 2000, Icarus, 143, 324

Harris, W. M., Scherb, F., Mierkiewicz, E. J., Oliversen, R. J., & Morgenthaler, J. P. 2002, ApJ, 578, 996

Haser, L. 1957, Bull. Soc. Roy. Sci. Liège, 43, 740

Huebner, W. F., Keady, J. J., & Lyon, S. P. 1992, Astrophys. Space Sci., 195, 1

Morgenthaler, J. P., *et al.* 2001, ApJ, 563, 451

Morgenthaler, J. P., Harris, W. M., Scherb, F., Roelser, F. L., Anderson, C. M., Doane, N. E., & Oliversen, R. J. 2002, Earth, Moon, Planets, 90, 77

Nee, J. B., & Lee, L. C. 1984, J. Chem. Phys., 81, 31

Roesler, F. L. 1974, in Methods of Experimental Physics, ed. N. P. Carleton, Vol. 12, part A (New York: Academic Press), 531

Scherb, F., *et al.* 1997, BAAS, 29, AAS/Division of Planetary Sciences Meeting 29, poster #32.01

Tozzi, G. P., Feldman, P. D., & Festou, M. C. 1998, A&A, 330, 753

van Dishoeck, E. F., & Dalgarno, A. 1984, Icarus, 59, 305

This preprint was prepared with the AAS LaTeX macros v5.0.